Khulna University Studies Special Issue ICSTEM4IR: 83-92, 2022

ORIGINAL ARTICLE

SCIENCE & ENGINEERING

DESIGN AND INVESTIGATION OF THREE-DIMENSIONAL POLARIZATION-INDEPENDENT POLYMER MACH-ZEHNDER INTERFEROMETERS AT 1550 NM

Noor Afsary[1], Md Omar Faruk Rasel[1,*], and Takaaki Ishigure[2]

[1]Physics Discipline, Khulna University, Khulna-9208, Bangladesh
[2]Faculty of Science and Technology, Keio University, Yokohama, 223-8522, Japan

KUS: ICSTEM4IR-22/0203

Manuscript submitted: August 12, 2022 Accepted: September 25, 2022

Abstract

We propose a Mach-Zehnder interferometer (MZI) which consists of a taper, a bending waveguide, and two symmetrical arms. The structure is realized with organic-inorganic hybrid polymer materials and analyzed by a commercially available RSoft CAD BeamPROP solver. We set the core width for input and output of the Mach-Zehnder interferometer at 6 μm for single-mode propagation. This interferometer shows an excess loss of 0.162 dB and has an efficiency of almost 96.4%. We also investigate the polarization dependency of this interferometer varying the beam incident angles from 0-30 degrees and this investigation suggests that this MZI shows polarization dependency when the light incident on the launched side of this MZI at 30° for transverse electric (TE) and transverse magnetic (TM) modes.

Keywords: Mach-Zehnder interferometer, Step-index profile, Beam propagation method, Polarization dependency, Numerical aperture, Polymer waveguide.

Introduction

The optical interconnect plays an important role to meet the growing global-bandwidth demand by transmitting the signal with the speed of light in high-performance computing systems (Taubenblatt, M. A., 2012) and data centers (Lu et al., 2019) over electrical counterparts. Meanwhile, polymer-based waveguides have shown much interest due to their easy fabrication on printed circuit boards (PCBs), low propagation loss, high flexibility, high-density wiring, and high bandwidth features for short-reach interconnects (Yu et al., 2021; Ishigure et al., 2010). Hence, various types of optically active and passive devices such as waveguides, couplers, interferometers, modulators, rings, etc.) are required for the development of photonic integrated circuits.

*Corresponding author: <ofr_ju@phy.ku.ac.bd>
DOI: https://doi.org/10.53808/KUS.2022.ICSTEM4IR.0203-se

For the application of complicated wiring, Mach-Zehnder Interferometer exhibits much interest by meeting several features such as switching (Krishnamurthy et al., 2014), multiplexing/demultiplexing (Ahmmed et al., 2021), sensors (El Shamy et al., 2019), and modulators (Hassanien et al., 2022), etc. in the optical communication system. Because of thermal stability, compact design, and high nonlinearity, symmetric Mach-Zehnder interferometer are especially effective for signal modulation. An MZI usually consists of two arms and is used to detect phase shifts between these two arms by splitting the light from a source and then by subjecting the phase shifts which are then guided into two paths, and then subjecting the phase shift, the light is being recombined. The phase shift is intentionally introduced for electro-optic modulators in one or both optical paths by modulating the refractive index. Hence, if we change the effective refractive index Δn_{eff}, it modifies the phase constant β of an optical wave with a free space wavelength of λ_0. However, if the differential phase shift is introduced between the two arms of the interferometer, the constructive or destructive interferences can be observed from the output. A phase shift of π can generate destructive interference where all light will be extinct; however identical phase shift can generate constructive interference resulting in maximum possible light out of the interferometer. Xiao et al., 2016 demonstrated polymer-based MZI for the applications of switching circuits, however, this device exhibits asymmetric structures. Lin et al., 2019 designed and fabricated an asymmetric polymer-based MZI sensor, however, the thickness of this device is 4 μm, which is comparatively higher and creates warpage during curing of the waveguides, resulting in high coupling loss.

In this paper, we have designed and analyzed a taper-based symmetric Mach-Zehnder interferometer, in which taper waveguides are inserted into its input and output cores. The structure of this MZI is optimized after investigating the following parameters such as input and output core width, length of S-bend waveguide, length of symmetric arms, and height and width of the tapered core. In addition, we investigate the normalized intensity, excess loss, and polarization-dependency for the TE and TM polarization at 1550 nm. The polarization effect can be applied in BPM by recognizing the electric field E as a vector.

Schematic Design and Analysis

The schematic design of the proposed MZI is shown in figure 1, which consists of three waveguide configurations: straight, taper, and S-bend. The straight waveguide is connected to the taper waveguides, and this taper waveguide is connected to the two S-bend waveguides, which can be introduced as a Y-splitter. Then, this Y-splitter is also connected to two symmetric waveguides. Finally, these two symmetric waveguides are connected to another two S-bend waveguides forming Y-combiner and can produce a single output. Light is launched into the input, which is connected to the taper. The width of the taper is varied from 6-12 μm. Here, the taper works as a splitter. After passing the taper, the guided light beam is divided into two segments and passes through the bending waveguide. It propagates to the symmetric arms, and the light is combined by a combiner and produces a single output. The cross-section of this MZI is shown in Figure 1(c).

The schematic presented in Figure 1 can be fabricated by the Imprint method (Abe et al., 2018). The fabrication details of the Imprint method can be illustrated in a couple of steps. First, the proposed core patterns are developed with photolithography on the photoresist, and these patterns are transferred to poly dimethyl siloxane (PDMS), and then the patterns are retransferred to the cladding monomer as the grooves of the cores. The under-cladding is cured and we remove the PDMS mold. Then, the core-pattern grooves are filled up with liquid core monomer and cured by UV light. Finally, the cladding monomer is coated over the core and the under-cladding as the over-cladding and cured UV light followed by post-backing.

DOI: https://doi.org/10.53808/KUS.2022.ICSTEM4IR.0203-se

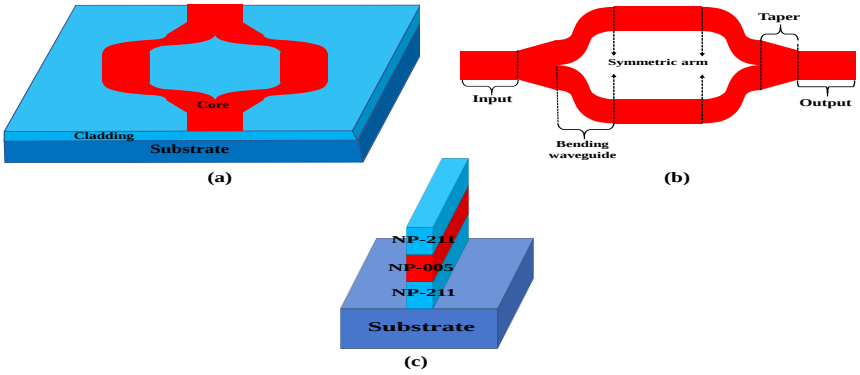

Figure 1. Schematic diagram of MZI:(a) 3D view, (b) top view, and (c) cross-section.

Materials and Method

This polymer-based Mach-Zehnder interferometer was developed by using organic-inorganic hybrid resins named SUNCONNECT(R) materials, which are supplied by Nissan Chemical Corporation Ltd. Japan. The core and cladding materials are NP-005 and NP-211, and the refractive indices of NP-005 (core) and NP-211 (cladding) are 1.575 and 1.567, respectively at 1550 nm. We select this material combination because these materials exhibit low propagation loss at 1550 nm due to their internal structural bonding. We design and develop this MZI waveguide by using the beam propagation method with a commercially available RSoft CAD BeamPROP solver. The index profile of this waveguide is step-index (SI) as shown in Figure 2, which shows that the uniform refractive index is uniformly distributed throughout the waveguide.

The configurations of the MZI can be studied using the transfer matrix model. If we represent each sub-component of this MZI as a vector quantity, the final output can be obtained by multiplying the individual matrices. The matrix formulation of the electric field outputs of the

Y-branch combiner is as follows:

$$\begin{bmatrix} E_{Y,O1} \\ E_{Y,O2} \end{bmatrix} = \begin{bmatrix} \sqrt{\epsilon_1} \\ \sqrt{\epsilon_2} \end{bmatrix} [E_1] \tag{1}$$

where E_1 is the electric field phasors of input, $E_{Y,O1}$ and $E_{Y,O2}$ are the output of both arms respectively. And the output power ratio of arm 1 is ϵ_1 and for the second arm, it is ϵ_2. The propagation is the arms of the MZI can be modeled by modifying the amplitude and the phase such as:

$$\begin{bmatrix} E_{Y,O1} \\ E_{Y,O2} \end{bmatrix} = \begin{bmatrix} \exp(-j\emptyset_1 - \frac{\alpha_1}{2} L_1) & 0 \\ 0 & \exp(-j\emptyset_2 - \frac{\alpha_2}{2} L_2) \end{bmatrix} \begin{bmatrix} E_{Iarm01} \\ E_{Iam02} \end{bmatrix} \tag{2}$$

where, $\emptyset_1$ and $\emptyset_2$ is the total phase shift in arm 1 and arm 2 and α_1 and α_2 is the optical propagation loss in the respective arms. And L_1 and L_2 are the total lengths of each arm. The terms E_{Iarm01} and E_{Iam02} are the input fields at the two arms of the interferometer, respectively. Thus, the intensity I of the interference patterns can be expressed as:

$$I = I_{core} + I_{clad} + 2\sqrt{I_{core} I_{clad}} \cos(\Phi) \tag{3}$$

where Φ is the total phase difference between the core and the cladding modes.

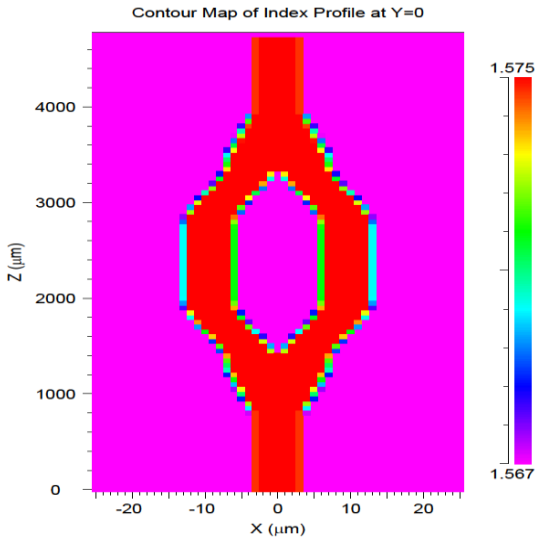

Figure 2. Index profile of SI Mach-Zehnder interferometer.

Structural Optimization

Since the input and output of this MZI are single-mode cores, the input and output waveguides follow the single-mode conditions, and the cut-off core width for these waveguides should be less than 7 μm (Rasel et al., 2019). The core width is an important parameter to attain the single-mode condition and we calculate the optimized core width for the input and output of this MZI after varying the core width in a range of 3-10 μm as a function of normalized intensity, as reported in Figure 3. From Figure 3, we can see that the normalized output intensity increases as the core width increases, and the maximum normalized output intensity is obtained, when the core width is 6 μm and the output intensity gradually decreases. Hence, we set the core width for the input and output cores as 6 μm.

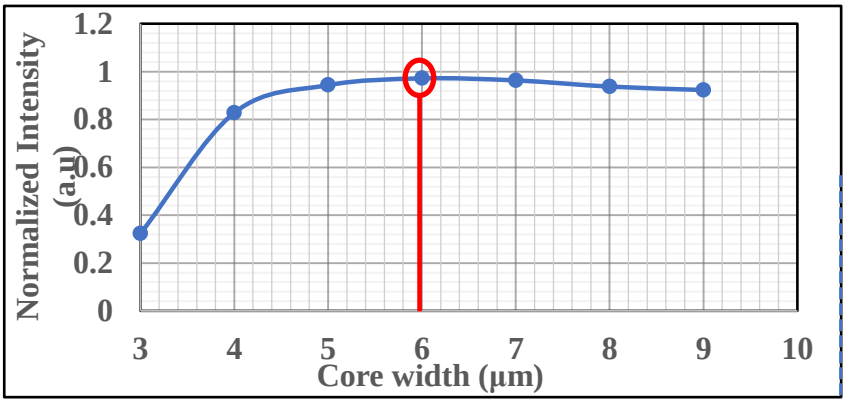

Figure 3. Output uniformity as a function of the core width.

DOI: https://doi.org/10.53808/KUS.2022.ICSTEM4IR.0203-se

To determine the suitable length for the S-bend waveguide of this MZI, we investigate a couple of simulation trials varying the length of the S-bend arm in a range of 100-1000 µm and record the output intensity. Then, we plot the output intensity as a function of bending arm's length, as introduced in Figure 4. From the graph, it is evident that the maximum output power increases as the increase of bending arm's length, and the maximum output intensity is obtained at 760 µm. Thus, we use the S-bend arm's length as 760 µm for this MZI design.

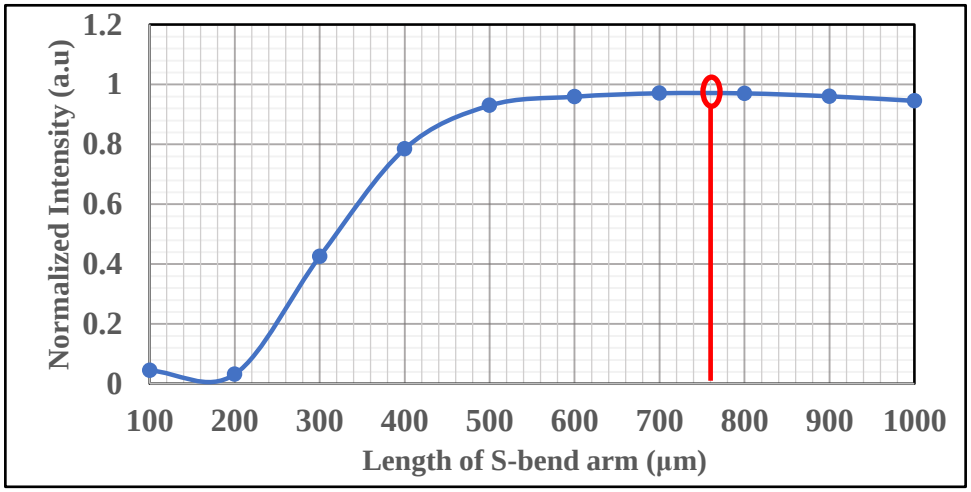

Figure 4. Output intensity depends on the length of the S-bend arm.

The length of the arms is one of the best parameters, which is responsible for shifting the phase of the input signal in MZI. Here, both arms are symmetric and we need to determine the suitable length of these symmetric arms.

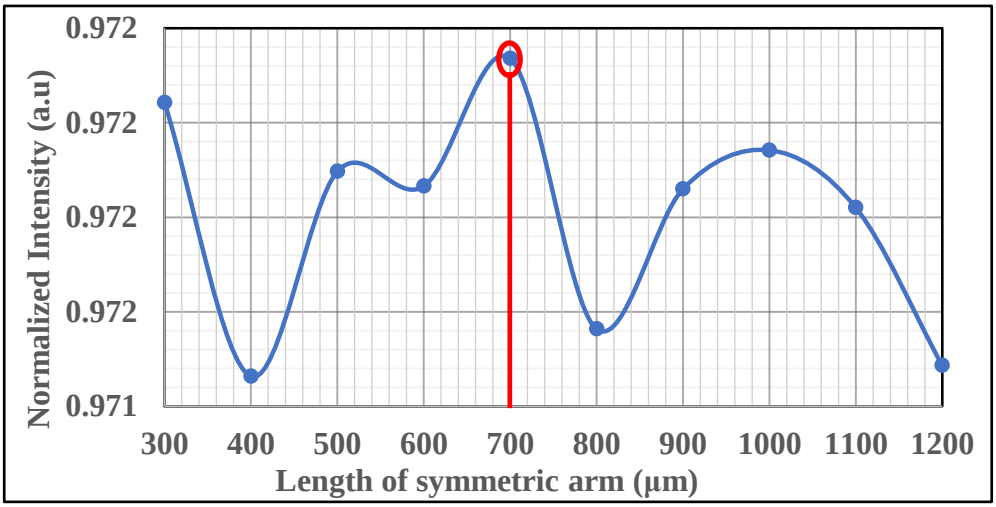

Figure 5. Output intensity depends on the length of the symmetric arms.

A straight waveguide does not vary too much for the step-index profile, however, we know in the modulation process, the slight change affects a lot. Hence, after several investigations, we plot the length of the symmetric arm in a range of 300 to 1200 μm for the SI profile, as introduced in Figure 5. From this Figure, it is obvious that the output normalized intensity is varied randomly according to the length of the arm. The maximum intensity is obtained when the length of the arm is 700 μm for the symmetric arms. Thus, we set the length for the symmetric arms as 700 μm. After investigating similar trials, we can determine the suitable height and width of the taper waveguides, which are included in this MZI structure. In addition, we also set the length of the input and output cores. Finally, we introduce the optimized parameters of this MZI waveguide in Table 1.

Table 1. Parameter's values for this MZI structure

Parameter's name	Value (μm)
Input/output core width	6
S-bend length	760
Symmetric arm length	700
Input/output length	800
Taper height	460
Taper width	6-12

After optimization of the parameter values, we can simulate this MZI waveguide at 1550 nm by using the RSoft CAD BeamPROP solver, and the performance of this MZI and its field distribution is shown in Figure 6.

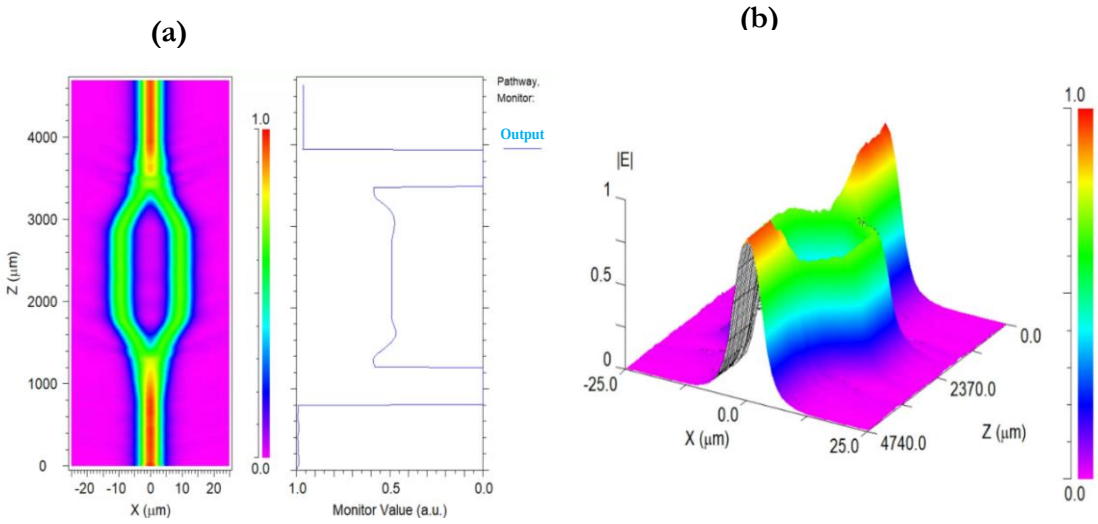

Figure 6. a) Simulation result for symmetric Mach-Zehnder interferometer. The intensity dramatically falls to zero when the light beam is launched at the tapered input and the intensity also increases from the taper's output, and b) 3D intensity patterns.

DOI: https://doi.org/10.53808/KUS.2022.ICSTEM4IR.0203-se

Results and Discussions

We investigate the light propagation through the symmetric polymer-based taper MZI waveguide. When no polarization is applied, the input light doesn't change, as shown in figure 8. As a result, the light first propagates through the input segment of this MZI waveguide and splits into two paths in the taper section. In the taper section, the intensity sharply falls and the intensity increases at the output of this taper section and then passes through the S-bend arm and moves directly to the symmetric arms of the MZI. After that, the intensity follows the reverse process of the Y-splitter and is combined in the output waveguide. The total output efficiency of this MZI waveguide is almost 96.4% at the waveguide length of 3990 μm and exhibits the same intensity throughout the output length.

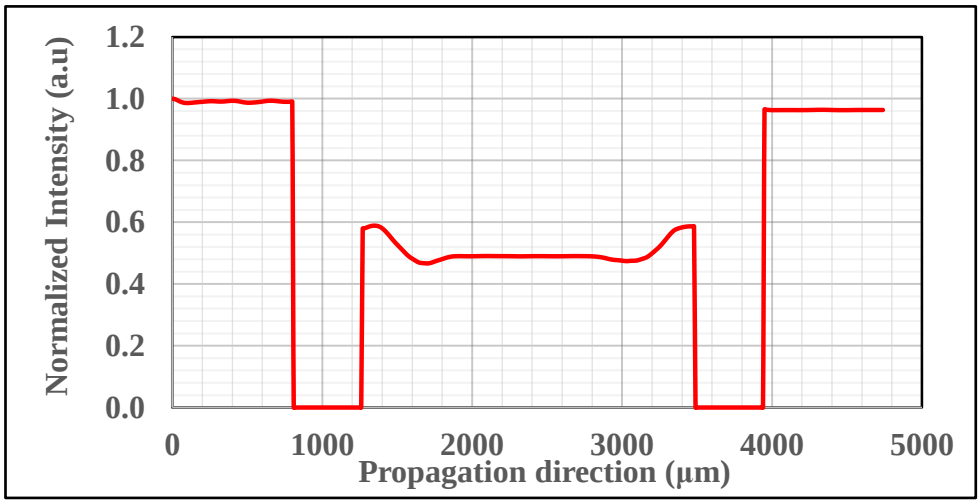

Figure 7. Light propagation through symmetric Mach-Zehnder.

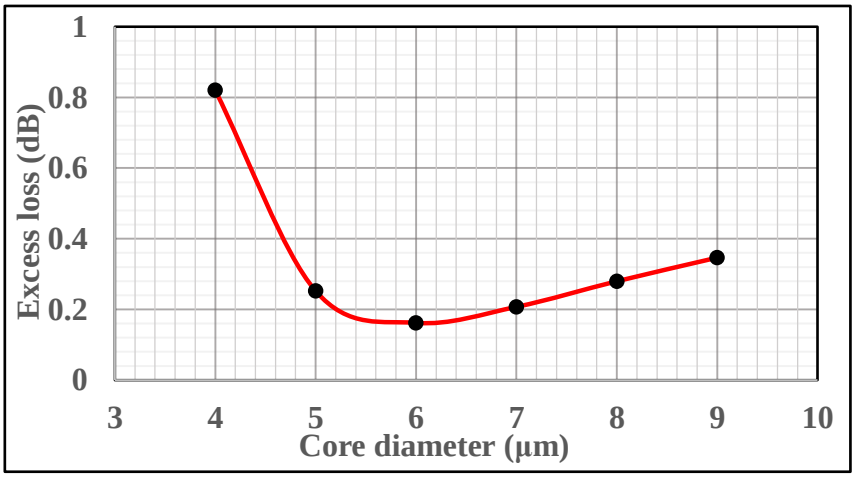

Figure 8. Excess loss for step-index symmetric MZI.

The excess loss (EL) is important to evaluate the performance of this MZI waveguide. Here, we measure the excess loss of this MZI waveguide following the equation (Soldano et al., 1995) in dB unit as follows:

$$EL = -10 \log 1 0 \left(\frac{\sum_{i=1}^{n} P_i}{P_0}\right) \quad (4)$$

here, i=1,2,3..... are the numbers of the output cores, P_i and P_0 are the power of input and output cores, respectively. The excess loss of the optimized symmetric taper-based MZI is shown in figure 8, where the variation of the excess loss is shown for core diameter. From Figure 8, it is evident that the low excess loss is obtained at the core diameter of 6 μm, and this symmetric MZI shows a minimum excess loss of 0.162 dB. When we apply polarization in the full vectorial method, we get transverse magnetic (TM) and transverse electric (TE) components. And, since the symmetric MZI is polarization-dependent, the light intensity almost jumps down to its half. Hence, the light propagation through this MZI is comparatively lower than that of light propagation without polarization. To reduce the loss factor due to polarization, we launch the light beam at different incidents and it is obvious that the input intensity changes varying the incident angles as mentioned in Figure 9.

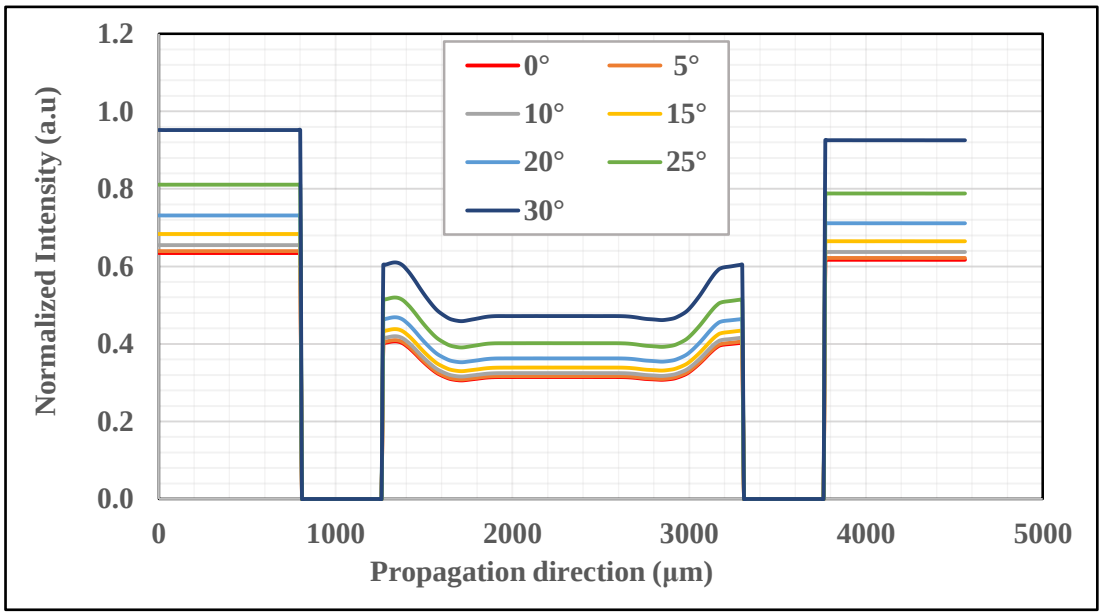

Figure 9. Polarization at various angles in the propagation direction of the MZI.

From Figure 9, we can see that due to difference input angles of 0°, 5°,10°,15°,20°,25°, and 30°, the intensities of input light are 0.635 a.u, 0.640, a.u, 0.655 a.u, 0.684 a.u,0.732 a.u, 0.811 a.u, and 0.952 a.u, and the maximum output intensity is obtained at 30° incident angle and it is 0.952 a.u for TE mode. This result suggests that this symmetric MZI exhibits polarization-independent when the light incident angle is 30°. We compare the results of our MZI device to other MZI devices published by other researchers as shown in Table 2, and we confirm that our proposed MZI waveguide exhibits excellent optical properties compared to the other MZI waveguides.

Table 2. Comparisons between the performances of MZI

Reference	Structure	Wavelength (nm)	Material	Efficiency	Loss (dB)	Polarization Angle
1	Y- Branch (Alam et al., 2021)	1550	Polymer	71 %	1.4	-
2	MZI (Zhang et al., 2021)	1550	SOI	>95%	0.03	-
3	MZI (Zhao et al., 2022)	1530–1600	SOI	>91%	0.6	-
4	Asymmetric MZI (Lin et al., 2019)	1550	Polymer	-	2.5	-
This paper	Symmetric MZI	1550nm	Polymer	96.4 %	0.162	30°

Conclusion

We have designed and demonstrated a symmetric Mach-Zehnder interferometer realized with polymer materials by using the beam propagation method. This interferometer exhibits high efficiency and it is almost 96.4%. The numerical analysis suggests that this MZI demonstrates a low excess loss of 0.162 dB. We also investigate the polarization dependency in this MZI varying the incident angles in a range of 0-30 degrees, and it is confirmed that this MZI exhibits polarization dependency at a 30^0 incident angle for TE mode. This numerical investigation of this MZI waveguide could be helpful to develop polarization-independent MZI waveguides in the research laboratory and industry.

Acknowledgment

The Authors would like to acknowledge BANBEIS, Ministry of Education, Bangladesh for providing a grant (ET20211588) partially to pursue this research.

References

Abe K., Oizumi Y., and Ishigure T. (2018). Low-loss graded-index polymer crossed optical waveguide with high thermal resistance. Opt. Express 26(4), 4512-4521.

Ahmmed, K. T., Chan, H. C., and Li, B. (2021). Three-mode multiplexer and demultiplexer based on the Mach-Zehnder interferometer. OSA Continuum, 4(5), 1519-1532.

Alam, M. K., Afsary, N., Rasel, M. O. F., and Ishigure, T. (2021). Multimode interference-based Y-branch polymer optical waveguide splitter: Design and Investigation," 2021 International Conference on Electronics, Communications and Information Technology (ICECIT), Khulna University, Bangladesh, 1-4. doi: 10.1109/ICECIT54077.2021.9641413.

El Shamy, R. S., Swillam, M. A., and Khalil, D. K. (2019). Mid-infrared integrated MZI gas sensor using suspended silicon waveguide. *Journal of Lightwave Technology*, 37(17), 4394-4400

Hassanien, A. E., Ghoname, A. O., Chow, Goddard, E. L., and Gong, S. (2022). Compact MZI modulators on thin film Z-cut lithium niobate. Opt. Express, 30(3), 4543-4552.

Ishigure, T. and Nitta, Y (2010). Polymer optical waveguide with multiple graded-index cores for on-board interconnects fabricated using soft-lithography. Opt. Express,18(13), 14191-14201.

Krishnamurthy, V., Chen, Y., and Wang, Q. (2014). MZI-semiconductor-based all-optical switch with switching gain. J. Lightwave Technol., 32(13), 2433-2439.

Lin, B., Yi, Y., Cao, Y., Lv, J., Yang, Y., Wang, F., Sun, X., Zhang, D. (2019). A polymer asymmetric Mach–Zehnder interferometer sensor model-based on electrode thermal writing waveguide technology. Micromachines 10, 628. https://doi.org/10.3390/mi10100628

Lu, Y. and Gu, H. (2019). Flexible and scalable optical interconnects for data centers: Trends and Challenges. IEEE Communications Magazine, 57(10), 27-33.

Rasel, O. F., and Ishigure, T. (2019). Circular core single-mode 3-dimensional crossover polymer waveguides fabricated with the Mosquito method. Opt. Express, 27(22), 32465-32479.

Soldano, L. B., and Pennings, E. C. M. (1995). Optical multi-mode interference devices based on self-imaging: principles and applications. J. Lightwave Technol. 13(4), 615-624.

Taubenblatt, M. A. (2012). Optical interconnects for high-performance computing. J. Lightwave Technol, 30, 448-457.

Xiao, Y., Hofmann, M., Wang, Z., Sherman, S., and Zappe, H. (2016). Design of all-polymer asymmetric Mach–Zehnder interferometer sensors. Appl. Opt. 55(13), 3566-3573.

Yu, S., Zuo, H., Gu, T. and Hu, J. (2021). A flexible polymer waveguide platform with low-loss optical interfaces. *2021 Conference on Lasers and Electro-Optics Europe & European Quantum Electronics Conference (CLEO/Europe-EQEC)*, 1-1, doi: 10.1109/CLEO/Europe-EQEC52157.2021.9541891.

Zhang, J., Zhang, Z., Ma, C., Chen, X., Liu, L., Zhao, W., Song, X., Zhang, H., Yu, Y., Chen, H., Yang, J. (2021). Ultra-compact and ultra-broadband polarization-insensitive Mach–Zehnder Interferometer in silicon-on-insulator platform for quantum internet application. Photonics 8, 455. https://doi.org/10.3390/photonics8100455.

Zhao, W., Liu, R., Peng, Y., Yi, X., Chen, H., and Dai, D. (2022). High-performance silicon polarization switch based on a Mach–Zehnder interferometer integrated with polarization-dependent mode converters. Nanophotonics, 11(10), 2293-2301. https://doi.org/10.1515/nanoph-2022-0022.